



Sepia officinalis'ten Kitin ve Kitosan: Ekstraksiyon ve Karakterizasyon Çalışması

Erkan UĞURLU ^{1*}, Önder DUYSAK ¹

¹Marine Science and Technology Faculty, Iskenderun Technical University, Iskenderun, Hatay / Türkiye

*E-mail: erkn.ugurlu@yahoo.com

Makale Bilgisi:

Geliş:

04/03/2024

Kabul Ediliş:

31/07/2024

Anahtar Kelimeler:

- Alternatif
- Biyojenik atık
- Yeşil biyoteknoloji
- Biyopolimer

Öz

İskenderun balık pazarından temin edilen *Sepia officinalis* kaynaklı mürekkep balığı kemiği, kitin (CT) ve kitosan (CS) üretiminde kullanıldı. Hem CT hem de CS'nin kimyasal yapısı ve fiziko-kimyasal özellikleri, Fourier-Dönüşümlü Kızılötesi (FTIR), X-Işını Kırınımı (XRD) ve Taramalı Elektron Mikroskopu (SEM) aracılığıyla kapsamlı bir şekilde karakterize edildi. Mürekkep balığı kemiğinden elde edilen CT ve CS verimleri sırasıyla $32.1 \pm 0.15\%$ ve $72.6 \pm 0.21\%$ olarak hesaplandı. FTIR spektrum analizi sonuçları, çeşitli bantlarda işlevsel grupların varlığını ortaya koyarak örneklerin CT ve CS olduğunu doğruladı. Deasetilasyon derecesi (DD) değeri, FTIR sonuçlarına göre %84,20 olarak belirlendi. Mürekkep balığı kemiğinden elde edilen CT'nin kristal indeks (CrI) değeri %60,13 olarak hesaplandı. SEM analizi, CT'nin yüzey morfolojisinde mikro-nano gözeneklerin ve mikro liflerin bulunduğunu, CS'nin ise pullu katmanlardan, mikro liflerden oluştuğunu ve oldukça gözenekli ve fibriller bir yapı sergilediğini ortaya çıkardı. Ticari öneme sahip ve yaygın olarak tüketilen *S. officinalis*'in sırt yüzgecinden bu biyopolimerler başarılı bir şekilde elde edildi. Deniz hayvanlarının kabuklarından elde edilen bu biyopolimerler, piller, mikrodalga elektroniği, ambalaj malzemeleri ve ilaç endüstrisi gibi çeşitli alanlarda alternatif ve yenilikçi çözümler sunan sürdürülebilir ve çevre dostu malzemeler olarak kullanılabilir.

Chitin and Chitosan from *Sepia officinalis*: Extraction and Characterization Study

Article Info

Received:

04/03/2024

Accepted:

31/07/2024

Keywords:

- Alternative
- Biogenic residual
- Green-biotechnology
- Biopolymer

Abstract

A cuttlebone sourced from *Sepia officinalis*, acquired from the Iskenderun fish market, served as the raw material for the extraction of chitin (CT) and chitosan (CS). The chemical structure and physico-chemical properties of both CT and CS were comprehensively characterized through Fourier-transform infrared (FTIR), X-ray Diffraction (XRD) and Scanning Electron Microscopy (SEM). The yields of CT and CS obtained from the cuttlebone of *S. officinalis* were calculated as $32.1 \pm 0.15\%$ and $72.6 \pm 0.21\%$, respectively. The results of FTIR spectrum analysis revealed the presence of functional groups at various bands, confirming the samples to be CT and CS. The deacetylation degree (DD) value was determined to be 84.20% based on the FTIR results. The crystalline index (CrI) of CT obtained from the cuttlebone was calculated as 60.13%. SEM analysis revealed that micro-pores, nano-pores, and microfibers were present in the surface morphology of chitin, while chitosan was found to consist of scaly layers, microfibers, and exhibited a highly porous and fibrillar structure. The biopolymers were successfully obtained from the dorsal fin of commercially important and widely consumed *S. officinalis*. These biopolymers derived from marine animal shells can be utilized as sustainable and environmentally friendly materials offering alternative and innovative solutions in various fields such as batteries, microwave electronics, packaging materials, and the pharmaceutical industry.

Atf bilgisi / Cite as: Uğurlu, E. & Duysak, Ö. (2024). Chitin and Chitosan from *Sepia officinalis*: Extraction and Characterization Study. Menba Journal of Fisheries Faculty, 10 (3), 1-13. DOI: 10.58626/menba.1447172.

INTRODUCTION

In the world, there are extensive aquatic areas and the marine animals inhabiting these vast regions are considered a renewable resource. The utilization of marine-derived biomaterials, particularly marine waste components, is of utmost importance for human well-being. Marine organisms constitute a significant source of bioactive natural products with unique structural and chemical properties not found in terrestrial animals (Ullah & Khan, 2023). Chitin (CT) and chitosan (CS) biopolymers, obtained from marine by-products such as mussel shells, shrimp shells, fish scales and cuttlebone, are utilized in various areas, including tissue engineering and the pharmaceutical industry (Alabaraoye et al., 2018). Chitin (CT), the second most abundant polysaccharide worldwide after cellulose, has attracted attention in the field of eco-friendly technology due to the increasing emphasis on biopolymers and bio-based polymers (Rudall & Kenchington 1973. These natural alternatives provide functionality and superior biodegradability compared to synthetic polymers (Hahn & Hennecke, 2023).

Chitosan (CS), obtained from chitin through deacetylation, is a naturally occurring polysaccharide. Deacetylation, which involves the removal of acetyl groups, is carried out at elevated temperatures and specific durations using strong alkalis. CS is distinguished by its non-toxic, bioabsorbable, compatible and degradable properties (Islam et al., 2020). Studies suggest that chitin (CT) and chitosan sourced from marine invertebrates globally demonstrate antitumor, anti-leukemia, antibacterial and antiviral activities (Islam et al., 2023; Ma et al., 2023; Nafary et al., 2023; Žigayová et al., 2023). The cuttlebone are natural sources containing chitin, and chitosan (CS) is obtained through processes of deproteinization, demineralization and deacetylation.

The cuttlebone, also known as the calcareous inner shell of *Sepia*, plays a vital role in cuttlefish buoyancy control in water due to its gas-filled structure (Le Pabic et al., 2017). Functioning as a highly porous and rigid floating reservoir within the cuttlefish body, cuttlebone is utilized in various applications, particularly in toothpaste production (Checa et al., 2015; Le Pabic et al., 2017). Furthermore, it functions as an absorbent for the uptake of metals from aqueous solutions. Recent studies have demonstrated its efficacy in eliminating significant pollutants, such as fluoride from drinking water and cobalt (II) from aqueous solutions (Ben Nasr et al., 2011; Kavisri et al., 2023).

β -chitin, a biopolymer, is extracted from this composite for diverse applications (Jung et al., 2018; Shushizadeh et al., 2015). Compared to α -chitin, β -chitin demonstrates increased solubility and swelling capacity (Birolli et al., 2016; Lamarque et al., 2007). This can be attributed to the weaker intermolecular hydrogen bonding arising from the parallel arrangement of the main chains. As a result, β -chitin is expected to possess a stronger affinity for various solvents and greater reactivity than α -chitin (Hasan et al., 2022). Recent research suggests that during the deacetylation process, β -chitin exhibits higher reactivity than α -chitin, indicating significant potential for participation in diverse chemical transformations (Rocha-Pino et al., 2007).

Although there are numerous cephalopod species, research tends to concentrate on taxonomic classification, growth patterns, biology, heavy metals and ink studies associated with this species (Duysak & Uğurlu, 2017, 2020; Duysak et al. 2023; Uğurlu et al. 2020; Queirós et al., 2023; Sajikumar et al., 2023; Tajika et al., 2021; Uğurlu et al., 2018; J. C. Xavier et al., 2018; J. Xavier & Chereil, 2021). Additionally, there are studies on chitin and chitosan conducted on cuttlebone obtained from various species (Arrouze et al., 2021; Ramasamy et al., 2014; Vino et al., 2012).

Considering this importance, the current study aimed to extract chitin (CT) and chitosan (CS) from the cuttlebone of *S. officinalis* obtained from Iskenderun fish market. Additionally, the study involved characterizing CT and CS biopolymers using SEM, FTIR and XRD techniques, as well as evaluating the yield, deacetylation degree, and solubility properties of CT and CS.

MATERIAL AND METHOD

Material

For this study, 10 samples of *S. officinalis* were collected from the Iskenderun fish market in June 2023. After dissection in the laboratory, the cuttlebones of *S. officinalis* were removed and underwent several washes with bidistilled water. Subsequently, the washed samples were dried in an oven at 60°C and ground (Figure 1). The dried shell powder samples were stored in a desiccator until further processing for chitin and chitosan production studies.

Figure 1. Cuttlebone of *S. officinalis* and after grinding process.

Methods

Extraction of CT and CS

The production of CT and CS was conducted in three stages, with each process followed by thorough washing with bidistilled water until reaching a neutral pH and subsequently left to dry at 50 °C for 24 hours. In the initial stage, the material was constantly stirred for 18 hours at 80 °C in the presence of 500 mL 1M NaOH (Takiguchi, 1991a). In the second stage, the deproteinated powder sample underwent treatment with 500 mL 1M HCl and was constantly stirred at RT for 18 hours (Takiguchi, 1991a). Finally, in the last stage, CT was subjected to deacetylation by continuous stirring at 100 °C for 4 hours, utilizing a 50% NaOH solution (Takiguchi, 1991b). After deacetylation, the chitosan was thoroughly washed with bidistilled water, dried at 50°C for 24 hours, and all obtained samples were stored in a desiccator until characterization studies were conducted.

Yields of CT and CS

The yields of the CT and CS obtained from the powders were calculated by correlating the weights of the raw shell powders with the weights of CT and CS taken later. The yields of CT and CS were calculated as described by Luo et al. (2019).

$$Y_{CT} = W_{CT} / W_{\text{Raw powder}} \times 100 \quad (1)$$

$$Y_{CS} = W_{CS} / W_{CT} \times 100 \quad (2)$$

where, Y: yield, W: weight, CT: chitin and CS: chitosan.

Solubility in acid solution

In order to assess the acid solubility of CT and CS powders derived from cuttlebone of *S. officinalis*, 1g of was measured and dissolved in 100 mL of a 1% acetic acid solution. The resulting solution was stirred and left at room temperature for 2 hours. Subsequently, it was filtered through pre-weighed filter paper, which was then dried. The dried paper along with the samples was weighed again. The percentage solubility was determined by analyzing the weight gain rate of the filter paper x100 (Nessa et al., 2011).

$$\text{Insoluble (g)} = \text{Final weight of filter paper (g)} - \text{initial weight of filter paper (g)} \quad (3)$$

$$\text{Insoluble (\%)} = (\text{Insoluble (g)}) / (\text{Sample weight (g)}) \times 100 \quad (4)$$

$$\text{Soluble (\%)} = 100 - \text{insoluble (\%)} \quad (5)$$

Fourier-Transform Infrared Spectroscopy (FTIR) Analysis

The CT and CS generated were subjected to characterization using a Jasco/FT/IR-6700 instrument equipped with ATR in the range of 400 to 4000 cm^{-1} , with the process for three replicates. The degree of deacetylation (DD) of the samples was defined following the method utilized by Brugnerotto et al. (2001). The A_{1320} represents the peak area at 1320 cm^{-1} , while the A_{1420} means the peak region at 1420 cm^{-1} , with A_{1320} related with the amide group and A_{1420} related with the amine group.

$$\% \text{ DA} = [(A_{1320} / A_{1420}) - 0.3822] / (0.03133) \quad (6)$$

$$\% \text{ DD} = 100 - \% \text{ DA} \quad (7)$$

where, DA = degree of acetylation.

X-Ray Diffraction (XRD) Analysis

XRD analysis was utilized to assess the crystallinity of both CT and CS. The patterns were recorded using a Malvern Panalytical EMPYREAN 3rd generation analytical instrument (UK) with Cu K α radiation ($\lambda = 1.5406 \text{ \AA}$, 40 kV, 30 mA). Data gathering took place with a scanning rate of 1 $^\circ$ /min across a scanning angle range spanning from 5 $^\circ$ to 40 $^\circ$. The crystalline index (I_{cr}) was ascertained using the formula suggested by Yuan et al. (2011).

$$I_{cr110} = [(I_{110} - I_{am}) / I_{am}] \times 100 \quad (8)$$

Here, I₁₁₀ represents the peak intensity of the (110) diffraction at $2\theta = 20^\circ$ and I_{am} denotes the signal from amorphous diffraction at $2\theta = 16^\circ$.

Scanning Electronic Microscopy (SEM)

To enhance the imaging quality of the CT and CS biopolymers derived from the samples, the surfaces of the samples were coated with gold-palladium using a Sputter Coater from the POLARON SC7620 brand. Following the coating process, surface morphology images were captured using a JEOL JSM-6380LA device using 15 kV.

RESULT AND DISCUSSION

In recent years, significant emphasis has been placed on the bioactivity of natural materials derived from marine flora and fauna, particularly marine animals. CT (chitin) and CS (chitosan) were extracted from the cuttlebone of *S. officinalis* and analyses were conducted to determine the deacetylation degree, crystalline index, solubility values, as well as SEM, FTIR and XRD characteristics of the CT and CS biopolymers from *S. officinalis*.

Yield of CT and CS

Numerous researchers have documented variations in CT (chitin) yield across different species. For instance, Chandumpai et al. (2004) reported CT yields of 36.06% for *Loligo lessoniana* and 36.55% for *L. formosana*. Vино et al. (2011) found a CT yield of 21% from cuttlebone of *S. aculeata*, while Al Sagheer et al. (2009) reported varying yields of CT from different sources, including *Metapenaeus affinis* (19.13%), *Penaeus semisulcatus* (16.75%), *Portunus pelagicus* male (20.80%), *P. pelagicus* female (20.14%), *Thenus orientalis* (21.26%) and cuttlefish (7.40%). Palpandi et al. (2009) determined yield of the CT from the squid *Doryteuthis sibogae gladius* as 33.02%. In this study, the yield of CT obtained from *S. officinalis* cuttlebone was determined to be 32.1 \pm 0.15%.

CT, despite being a polymer, exhibits insolubility in water, limiting its widespread application. To enhance solubility and broaden its utility, numerous CT derivatives have been developed, with CS (chitosan) serving as a base material, representing the deacetylated form of CT. Researchers have explored CT extraction from various sources and notable efforts include the following:

- The CS yields from the shell, claw and legs of the Portunid crab *Scylla tranquebarica* were reported as 6.59%, 4.12% and 8.42%, respectively (Thirunavukkarasu & Shanmugam, 2009).
- The CS yields derived from the CT of *L. lessiana*, *L. formosana* and *P. monodon* were reported by Chandumpai et al. (2004) as 77.55%, 77.21% and 78.23%, respectively.
- Oduor-Odeto et al. (2005) reported CS yields obtained from CT of prawns, crabs, and lobsters as 75.1%, 74.6% and 74.3%, respectively.
- The percentage yield of CS from the chitinous material of various cephalopod sources was reported as 15% in *Sepia prashadi*, 15% in *Sepiella inermis*, 18.75% in *Sepioteuthis lessoniana* gladius and 21% in *S. aculeata* (Seedeve et al., 2017; Subhpradha et al., 2013; Vairamani et al., 2013; Vino et al., 2011).

In this study, the yield of CS obtained from the cuttlebone of *S. officinalis* was recorded as 72.6±0.21%. This rate was found to be higher than the yields of cuttlefish *S. inermis*, *S. prashadi*, *S. aculeata* and squid *S. lessoniana*. These variations are attributed to differences in species or distinct processing methods.

Solubility

The solubility of CT and CS biopolymers derived from the cuttlebone of *S. officinalis* in 1% acetic acid was calculated. The results revealed that the solubility of the cuttlebone CT biopolymer is 37.67±2.06%. Additionally, the cuttlebone CS biopolymer demonstrated a solubility value of 85.24±2.55%. Comparative studies by Demir et al. (2016) and Uğurlu and Duysak (2023) reported solubility values of CS obtained from shells in acetic acid as 99.29±0.001% and 85.26±1.55% to 88.06±2.23%, respectively. A high solubility of the CS biopolymer in acetic acid indicates a deacetylation degree of at least 85% (Hossain et al., 2014). Uğurlu and Duysak (2023) calculated the %DA and %DD values of CT biomaterials derived from the shell and spines of sea urchins as %15.8 and %14.20, respectively, while that of CS was calculated as %84.19-%85.80.

FTIR Analysis

FTIR characterization of the CT derived from cuttlebone was carried out using the Jasco/FT/IR-6700 device within the frequency range of 4000-400 cm⁻¹. Figure 2 depicts that the absorption patterns in the spectrum closely mirror those documented in the literature, confirming the formation of high-quality CT biopolymers. Table 1 showed that the absorption bands of CT prepared from cuttlebone were similar to those of standard chitosan (Kaya et al., 2015).

A thorough analysis of the FTIR data reveals characteristic bands specific to cuttlebone CT. In Figure 2, absorption peaks for cuttlebone CT are observed at 3407.61 cm⁻¹. These peaks indicate the stretching and vibrating of aliphatic O-H, with greater prominence in the CT spectrum. The spectrum bands of CT obtained from cuttlebone at 2938.39 cm⁻¹ represent the C-H vibration of -CH₃. Peaks at 1659.45 cm⁻¹ indicate the stretching and vibration of the carbonyl group C=O from acetamide (-NHCOCH₃).

Additional distinctive absorptions of the CT biopolymer derived from cuttlebone are noted at 1639.19 cm⁻¹ and 1443.45 cm⁻¹, indicating the bending vibration of -NH and the stretching vibration of -CN from the acetamide group.

Figure 2. FTIR bands of chitin (CT) and chitosan (CS) from cuttlebone of *S. officinalis*.

Moreover, the spectral peaks of CT from cuttlebone at 1063.55 cm⁻¹ indicate the stretching vibration associated with the -C-O-C of the glucosamine ring. The absorption peak at 856.24 cm⁻¹ serves as a characteristic peak for β-1,4 glycosidic bonds, signifying ring stretch. The presence of α-chitin in the cuttlebone is identified in this spectrum. Several researchers have observed that the distinctive bonding arrangement between α-chitin and β-chitin results in the splitting of the amide I band at 1660 cm⁻¹ in the α-chitin spectrum (Al Sagheer et al., 2009; Lavall et al., 2007). FTIR analysis has determined that the CT biopolymers obtained from the cuttlebone exhibit similarity to commercial CT (Palpandi et al., 2009).

Table 1. Comparison of significant peak wavenumbers in the FTIR spectrum of CT obtained from the cuttlebone of *S. officinalis* and commercial CT.

The synthesized CS samples underwent FTIR analysis and the results are illustrated in Figure 2. It has been observed that the spectrum of CS synthesized from *S. officinalis* cuttlebone closely resembles the commercial chitosan reported by Kaya et al. (2013). The FTIR peaks for cuttlebone CS are identified at 3352.63 cm⁻¹ (angular deformation of OH in the CS structure), 2938.02 cm⁻¹ (-CH stretching), 1652.69 cm⁻¹ (vibration modes of amide I), 1593.87 cm⁻¹ (-NH₂ bending vibration in the amino group), 1443.45 cm⁻¹ (vibration OH, CH in the ring), 1396.21 cm⁻¹ (-NH primary, secondary and tertiary bonds) and 1083 cm⁻¹ (C-O stretching in acetamide), as shown in Figure 2. Various research groups, including Al Sagheer et al. (2009), Si Trung and Bao (2015) and Younes and Rinaudo (2015) have reported similar bands for CS at 3441 cm⁻¹, 2909 cm⁻¹, 2808 cm⁻¹, 1633 cm⁻¹, 1603 cm⁻¹, 1593 cm⁻¹, 1412 cm⁻¹, 1352 cm⁻¹ and 1030 cm⁻¹. Furthermore, the FTIR results of the CS biopolymers in this study exhibit similarity to the standard chitosan results in the study conducted by Palpandi et al. (2009).

The FTIR spectra of the standard CS sample exhibited different bands at 3356 cm^{-1} , 2921 cm^{-1} , 1652 cm^{-1} , 1586 cm^{-1} , 1375 cm^{-1} and 1021 cm^{-1} (Kaya et al., 2013; Palpandi et al., 2009). The comparison of FTIR results between synthesized CS and a commercial chitosan sample confirms that these materials serve as excellent sources of CS and the synthesized material closely resembles the commercial chitosan reported by Kaya et al. (2013). The FTIR analysis has substantiated the successful extraction of CT and CS from *S. officinalis* cuttlebone, with the observed FTIR bands closely aligning with the literature (Chandumpai et al., 2004; Hasan et al., 2022; Kaya et al., 2013, 2015; Ramasamy et al., 2014; Uğurlu & Duysak, 2023; Vino et al., 2012).

Table 2. Comparison of significant peak wavenumbers in the FTIR spectrum of chitosan obtained from the cuttlebone of *S. officinalis* and commercial chitosan.

The degree of acetylation of the materials obtained from cuttlebone was determined through FTIR analysis. The absorbance method within the FTIR analysis was utilized to compute the %DA (degree of acetylation) and %DD (degree of deacetylation) for *S. officinalis* cuttlebone. A %DA value below 60% signifies CT, while a %DD above 60% indicates CS (Rinaudo, 2006). The calculation of DD and DA in *S. officinalis* was performed using the absorbance mode of the FTIR spectra. The calculated values for %DA and %DD for CT and CS extracted from *S. officinalis* cuttlebone were 15.80% and 84.20%, respectively. In comparison, Öğretmen et al. (2022) stated that the %DD of CS from pink shrimp (*Parapenaeus longirostris*) was 81%. Furthermore, Alabaraoye et al. (2018) reported varying percentages of %DA for CT materials obtained from mussel (91%), oyster (85.62%), shrimp (51.61%) and crab (69.4%). The differences observed in these results between the two studies and our current investigation are likely attributed to species variations and differences in experimental procedures.

XRD Analysis

The X-ray diffraction patterns of CT and CS extracted from *S. officinalis* cuttlebone are illustrated in Figure 3. The figure indicates the presence of CaCO_3 (calcite) and CT. The XRD analysis conducted in this study reveals the extraction of α -chitin. In the XRD analysis of cuttlebone CT, 14 crystal reflection peaks within the 5-90° range were observed, with the ten most prominent peaks at 20.10°, 22.30°, 29.20°, 30.70°, 31.40°, 32.05°, 39.70°, 42.80°, 44.60° and 49.20° (Figure 3). The highest peak reflection was noted between 20-25° at 2θ (1160° count s^{-1}).

In the XRD analysis of cuttlebone CS, 15 peaks were detected, with the six largest peaks at 12.70°, 20.55°, 26.30°, 28.80°, 29.20° and 35.40°. The most significant peak for CS was identified at 2θ between 20-30° (1090° count s^{-1}) (Figure 3). Previous studies have confirmed the existence of two identical peaks around 10° and 20° for shell powders exhibiting different degrees of deacetylation, which have been attributed to species or regional variations (Kumari et al., 2015; Trung et al., 2006).

Figure 3. Comparison of X-ray power diffractograms of chitin (CT) and chitosan (CS) from cuttlebone of *S. officinalis*.

The crystalline index (Icr) of CT extracted from *S. officinalis* cuttlebone was determined to be 60.13%. In contrast, Uğurlu and Duysak (2023) reported Icr values for chitin (CT) obtained from *Diadema setosum* testa and spines as 68% and 67%, respectively. Dahmane et al. (2014) reported Icr value of 93.67% for CT extracted from *Parapenaeus longirostris* shells. Cárdenas et al. (2004) reported varying Icr values for CT obtained from different sources including shrimp, lobster, crab, king crab and squid species, ranging from 66.3% to 82.7%. Ibitoye et al. (2018) determined Icr value of 88.02% for CT obtained from house cricket (*Brachytrupes portentosus*). The wide range of Icr values observed across these studies may be attributed to differences in species, extraction methods and the purity of the materials used.

SEM Analysis

The morphology of CT and CS obtained from cuttlefish bone was examined using SEM. Images with two different magnifications and from different regions are presented in Figure 4. SEM imaging reveals that CT extracted from cuttlebone consists of microfibrils along with micropores and nanopores in surface images (Figure 4a, b). Figure 4b provides a closer look at the inner matrix of nanofibers. The presence of numerous surface pores affirms the excellent porosity of this marine biomaterial. The extracted CS exhibits layers of flakes, microfibrils and a highly porous structure, observable in various areas. In certain sections of CS, distinct fibril structures are evident. Upon closer magnification in specific parts of the CS, the presence of fibrillar sheet scales is observed, reminiscent of findings in Yen et al. (2009) study on CS from crab and cuttlefish (*Sepia kobeensis*) (Ramasamy et al., 2014).

Figure 4. SEM images of chitin (CT) and chitosan (CS) from cuttlebone of *Sepia officinalis*: A, B) CT from cuttlebone, C, D) CS from cuttlebone.

CONCLUSION

In conclusion, this study has focused on determining the physicochemical properties of chitin (CT) and chitosan (CS) samples obtained from cuttlebone of *S. officinalis*, and on FTIR, XRD, and SEM analyses. The findings indicate that the extracted CT from cuttlebone is in the alpha (α) form, featuring a fine nanofiber structure with slight nano-porosity. The chitin and chitosan yields obtained from cuttlebone of *S. officinalis* were calculated as 32.1±0.15% and 72.6±0.21%, respectively. The degree of deacetylation was created to be 15.80% of chitin, while the degree of deacetylation of chitosan was 84.20%. The solubility of chitosan from cuttlebone was 85.24±2.55%. The CrI % of cuttlebone was found to be 60.13%. These biomaterials hold promising potential as alternatives in various industrial sectors such as petroleum, pharmaceuticals, medicine, textiles, and agriculture. The

unique properties revealed through this study contribute to the potential applications of these marine-derived biomaterials, opening avenues for further exploration and utilization in diverse industrial areas.

COMPLIANCE WITH ETHICAL STANDARDS

Ethical Approval

Authors declare that ethical approval is not required for this type of study.

Declarations

Authors declare that ethical approval is not required for this type of study.

Consent to Participate

It is not applicable for this study.

Consent to Publication

It is not applicable for this study.

Competing Interests

The authors have no relevant financial or non-financial interests to disclose.

Availability of Data and Materials

The datasets generated during the current study are not publicly available but are available from the corresponding author on reasonable request.

Acknowledgment

I would like to thank Cansev Genç for the support provided in laboratory studies.

Funding

The author declares that no funds, grants, or other support were received during the preparation of this manuscript.

REFERENCES

- Al Sagheer, F. A., Al-Sughayer, M. A., Muslim, S., & Elsabee, M. Z. (2009). Extraction and characterization of chitin and chitosan from marine sources in Arabian Gulf. *Carbohydrate Polymers*, 77: 410–419. <https://doi.org/10.1016/j.carbpol.2009.01.032>
- Alabaraoye, E., Achilonu, M., & Hester, R. (2018). Biopolymer (Chitin) from Various Marine Seashell Wastes: Isolation and Characterization. *Journal of Polymers and the Environment*, 26(6): 2207–2218. <https://doi.org/10.1007/s10924-017-1118-y>
- Arrouze, F., Desbrieres, J., Lidrissi-hassani, S., & Tolaimate, A. (2021). Investigation of β -chitin extracted from cuttlefish: Comparison with squid β -chitin. *Polymer Bulletin*, 78: 1–21. <https://doi.org/10.1007/s00289-020-03466-z>
- Ben Nasr, A., Walha, K., Charcosset, C., & Ben Amar, R. (2011). Removal of fluoride ions using cuttlefish bones. *Journal of Fluorine Chemistry*, 132(1): 57–62. <https://doi.org/10.1016/j.jfluchem.2010.11.006>
- Birrolli, W. G., de Moura Deleuzuk, J. A., & Campana-Filho, S. P. (2016). Ultrasound-assisted conversion of alpha-chitin into chitosan. *Applied Acoustics*, 103: 239–242.
- Brugnerotto, J., Lizardi-Mendoza, J., Goycoolea, F., Argüelles-Monal, W., Desbrieres, J., & Rinaudo, M. (2001). An infrared investigation in relation with chitin and chitosan characterization. *Polymer*, 42: 3569–3580. [https://doi.org/10.1016/S0032-3861\(00\)00713-8](https://doi.org/10.1016/S0032-3861(00)00713-8)
- Cárdenas, G., Cabrera, G., Taboada, E., & Miranda, S. P. (2004). Chitin characterization by SEM, FTIR, XRD, and ¹³C cross polarization/mass angle spinning NMR. *Journal of Applied Polymer Science*, 93(4): 1876–1885. <https://doi.org/10.1002/app.20647>
- Chandumpai, A., Singhpibulporn, N., Faroongsarng, D., & Sornprasit, P. (2004). Preparation and physico-chemical characterization of chitin and chitosan from the pens of the squid species *Loligo lessoniana* and *Loligo formosana*. *Carbohydrate Polymers*, 58(4): 467–474. <https://doi.org/10.1016/j.carbpol.2004.08.015>
- Checa, A. G., Cartwright, J. H. E., Sánchez-Almazo, I., Andrade, J. P., & Ruiz-Raya, F. (2015). The cuttlefish *Sepia officinalis* (Sepiidae, Cephalopoda) constructs cuttlebone from a liquid-crystal precursor. *Scientific Reports*, 5(1): 11513. <https://doi.org/10.1038/srep11513>

- Dahmane, E. M., Taourirte, M., Eladlani, N., & Rhazi, M. (2014). Extraction and Characterization of Chitin and Chitosan from *Parapenaeus longirostris* from Moroccan Local Sources. *International Journal of Polymer Analysis and Characterization*, 19(4): 342–351. <https://doi.org/10.1080/1023666X.2014.902577>
- Demir, D., Öfkeli, F., Ceylan, S., & Bölgen, N. (2016). Extraction and Characterization of Chitin and Chitosan from Blue Crab and Synthesis of Chitosan Cryogel Scaffolds. *Journal of the Turkish Chemical Society, Section A: Chemistry*, 3(3): 131–144. <https://doi.org/10.18596/jotcsa.00634>
- Duysak, Ö., & Uğurlu, E. (2017). Metal accumulations in different tissues of cuttlefish (*Sepia officinalis* L., 1758) in the Eastern Mediterranean coasts of Turkey. *Environmental Science and Pollution Research*, 24(10): 9614–9623. <https://doi.org/10.1007/s11356-017-8685-2>
- Duysak, Ö., & Uğurlu, E. (2020). Heavy Metal Accumulation in Different Tissues of Cuttlefish (*Sepia officinalis* L., 1758) in İskenderun Bay. *Journal of Anatolian Environmental and Animal Sciences*, 5(4): 556–562. <https://doi.org/10.35229/jaes.750466>
- Duysak, Ö., Kılıç, E., Uğurlu, E., & Doğan, S. (2023). Metal toxicity risk of commercial cephalopod species and public health concerns. *Regional Studies in Marine Science*, 66: 103141. <https://doi.org/10.1016/j.rsma.2023.103141>
- Hahn, S., & Hennecke, D. (2023). What can we learn from biodegradation of natural polymers for regulation? *Environmental Sciences Europe*, 35(1): 50. <https://doi.org/10.1186/s12302-023-00755-y>
- Hasan, S., Boddu, V. M., Viswanath, D. S., & Ghosh, T. K. (2022). Preparation of Chitin and Chitosan. In S. Hasan, V. M. Boddu, D. S. Viswanath, & T. K. Ghosh (Eds.), *Chitin and Chitosan: Science and Engineering* (pp. 17–50). Springer International Publishing. https://doi.org/10.1007/978-3-031-01229-7_2
- Hossain, M. S., Iqbal, A., Hossain, M. S., & Iqbal, A. (2014). Production and characterization of chitosan from shrimp waste. *Journal of the Bangladesh Agricultural University*, 12(1): 158–160. <https://doi.org/10.22004/AG.ECON.209911>
- Ibitoye, E. B., Lokman, I. H., Hezme, M. N. M., Goh, Y. M., Zuki, A. B. Z., & Jimoh, A. A. (2018). Extraction and physicochemical characterization of chitin and chitosan isolated from house cricket. *Biomedical Materials*, 13(2): 025009. <https://doi.org/10.1088/1748-605X/aa9dde>
- Islam, Md. M., Islam, R., Mahmudul Hassan, S. M., Karim, Md. R., Rahman, M. M., Rahman, S., Nur Hossain, Md., Islam, D., Aftab Ali Shaikh, Md., & Georghiou, P. E. (2023). Carboxymethyl chitin and chitosan derivatives: Synthesis, characterization and antibacterial activity. *Carbohydrate Polymer Technologies and Applications*, 5: 100283. <https://doi.org/10.1016/j.carpta.2023.100283>
- Islam, Md. M., Shahrzaman, Md., Biswas, S., Nur Sakib, Md., & Rashid, T. U. (2020). Chitosan based bioactive materials in tissue engineering applications-A review. *Bioactive Materials*, 5(1): 164–183. <https://doi.org/10.1016/j.bioactmat.2020.01.012>
- Jung, H.-S., Kim, M. H., Shin, J. Y., Park, S. R., Jung, J.-Y., & Park, W. H. (2018). Electrospinning and wound healing activity of β -chitin extracted from cuttlefish bone. *Carbohydrate Polymers*, 193: 205–211. <https://doi.org/10.1016/j.carbpol.2018.03.100>
- Kavisri, M., Abraham, M., Namasivayam, S. K. R., Aravindkumar, J., Balaji, D., Sathishkumar, R., Sigamani, S., Srinivasan, R., & Moovendhan, M. (2023). Adsorption isotherm, kinetics and response surface methodology optimization of cadmium (Cd) removal from aqueous solution by chitosan biopolymers from cephalopod waste. *Journal of Environmental Management*, 335: 117484. <https://doi.org/10.1016/j.jenvman.2023.117484>
- Kaya, M., Erdogan, S., Mol, A., & Baran, T. (2015). Comparison of chitin structures isolated from seven Orthoptera species. *International Journal of Biological Macromolecules*, 72: 797–805. <https://doi.org/10.1016/j.ijbiomac.2014.09.034>
- Kaya, M., Tozak, K. Ö., Baran, T., Sezen, G., & Sargin, I. (2013). Natural porous and Nano fiber chitin structure from *Gammarus argaeus* (Gammaridae Crustacea). *EXCLI Journal*, 12: 503–510. <https://doi.org/10.17877/DE290R-7353>
- Kumari, S., Rath, P., Annamareddy, S., & Tiwari, T. N. (2015). Extraction and characterization of chitin and chitosan from fishery waste by chemical method. *Environmental Technology & Innovation*, 3. <https://doi.org/10.1016/j.eti.2015.01.002>
- Lamarque, G., Chaussard, G., & Domard, A. (2007). Thermodynamic aspects of the heterogeneous deacetylation of β -chitin: Reaction mechanisms. *Biomacromolecules*, 8(6): 1942–1950.
- Lavall, R., Assis, O., & Campanafilho, S. (2007). β -Chitin from the pens of *Loligo* sp.: Extraction and characterization. *Bioresource Technology*, 98(13): 2465–2472. <https://doi.org/10.1016/j.biortech.2006.09.002>
- Le Pabic, C., Marie, A., Marie, B., Percot, A., Bonnaud-Ponticelli, L., Lopez, P. J., & Luquet, G. (2017). First proteomic analyses of the dorsal and ventral parts of the *Sepia officinalis* cuttlebone. *Journal of Proteomics*, 150: 63–73. <https://doi.org/10.1016/j.jprot.2016.08.015>

- Luo, Q., Wang, Y., Han, Q., Ji, L., Zhang, H., Fei, Z., & Wang, Y. (2019). Comparison of the physicochemical, rheological, and morphologic properties of chitosan from four insects. *Carbohydrate Polymers*, 209: 266–275. <https://doi.org/10.1016/j.carbpol.2019.01.030>
- Ma, B., Zhang, J., Mi, Y., Miao, Q., Tan, W., & Guo, Z. (2023). Preparation of imidazole acids grafted chitosan with enhanced antioxidant, antibacterial and antitumor activities. *Carbohydrate Polymers*, 315: 120978. <https://doi.org/10.1016/j.carbpol.2023.120978>
- Nafary, A., Mousavi Nezhad, S., & Jalili, S. (2023). Extraction and characterization of chitin and chitosan from *Tenebrio Molitor* beetles and investigation of its antibacterial effect against *Pseudomonas aeruginosa*. *Advanced Biomedical Research*, 12(1): 96. https://doi.org/10.4103/abr.abr_205_22
- Nessa, F., Masum, S. M., Asaduzzaman, M., Roy, S., Hossain, M., & Jahan, M. (2011). A Process for the Preparation of Chitin and Chitosan from Prawn Shell Waste. *Bangladesh Journal of Scientific and Industrial Research*, 45(4): 323–330. <https://doi.org/10.3329/bjsir.v45i4.7330>
- Oduor-Odeto, P. M., Struszezyk, M. H., & Peter, M. G. (2005). Characterisation of Chitosan from Blowfly Larvae and Some Crustacean Species from Kenyan Marine Waters Prepared Under Different Conditions. *Western Indian Ocean Journal of Marine Science*, 4(1): Article 1. <https://doi.org/10.4314/wiojms.v4i1.28478>
- Öğretmen, Ö. Y., Karsli, B., & Çağlak, E. (2022). Extraction and Physicochemical Characterization of Chitosan from Pink Shrimp (*Parapenaeus longirostris*) Shell Wastes. *Journal of Agricultural Sciences*, 28(3): Article 3. <https://doi.org/10.15832/ankutbd.861909>
- Palpandi, C., Shanmugam, V., & Shanmugam, A. (2009). Extraction of chitin and chitosan from shell and operculum of mangrove gastropod *Merita (Dostia) crepidularia* Lamarck. *International Journal of Medicine and Medical Sciences*, 1(5): 198–205.
- Queirós, J. P., Bartolomé, A., Piatkowski, U., Xavier, J. C., & Perales-Raya, C. (2023). Age and growth estimation of Southern Ocean squid *Moroteuthopsis longimana*: Can we use beaks collected from predators' stomachs? *Marine Biology*, 170(1): 10. <https://doi.org/10.1007/s00227-022-04156-2>
- Ramasamy, P., Subhadrappa, N., Shanmugam, V., & Shanmugam, A. (2014). Extraction, characterization and antioxidant property of chitosan from cuttlebone *Sepia kobeensis* (Hoyle 1885). *International Journal of Biological Macromolecules*, 64: 202–212. <https://doi.org/10.1016/j.ijbiomac.2013.12.008>
- Rinaudo, M. (2006). Chitin and chitosan: Properties and applications. *Progress in Polymer Science*, 31(7): 603–632. <https://doi.org/10.1016/j.progpolymsci.2006.06.001>
- Rocha-Pino, Z., Shirai, K., Arias, L., & Vázquez, H. (2007). Effect of water quality and particle size on the production of chitosan from β -chitin isolated from jumbo squid processing wastes (*Dosidicus gigas*). *Revista Mexicana de Ingeniería Química*, 7(3): 299–307.
- Rudall, K. M., & Kenchington, W. (1973). The Chitin System. *Biological Reviews*, 48: 597–633. <https://doi.org/10.1111/j.1469-185X.1973.tb01570.x>
- Sajikumar, K. K., Laxmilatha, P., Vargheese, S., Pranav, P., Venkatesan, V., Vidya, R., Alloyicious, P. S., Joy, K. M. J., & Sasikumar, G. (2023). Hawaiian flying squid *Nototodarus hawaiiensis* (Cephalopoda: Ommastrephidae) in the Arabian Sea: range extension, age, and growth. *Marine Biodiversity*, 53(1): 15. <https://doi.org/10.1007/s12526-022-01325-w>
- Seedevi, P., Moovendhan, M., Vairamani, S., & Shanmugam, A. (2017). Evaluation of antioxidant activities and chemical analysis of sulfated chitosan from *Sepia prashadi*. *International Journal of Biological Macromolecules*, 99: 519–529. <https://doi.org/10.1016/j.ijbiomac.2017.03.012>
- Shushizadeh, M. R., Pour, E. M., Zare, A., & Lashkari, Z. (2015). Persian gulf β -chitin extraction from *sepia pharaonis* sp. Cuttlebone and preparation of its derivatives. *Bioactive Carbohydrates and Dietary Fibre*, 6(2): 133–142. <https://doi.org/10.1016/j.bcdf.2015.09.003>
- Si Trung, T., & Bao, H. N. D. (2015). Physicochemical Properties and Antioxidant Activity of Chitin and Chitosan Prepared from Pacific White Shrimp Waste. *International Journal of Carbohydrate Chemistry*, 2015: 1–6. <https://doi.org/10.1155/2015/706259>
- Subhadrappa, N., Ramasamy, P., Shanmugam, V., Madheswaran, P., Srinivasan, A., & Shanmugam, A. (2013). Physicochemical characterisation of β -chitosan from *Sepioteuthis lessoniana* gladius. *Food Chemistry*, 141(2): 907–913. <https://doi.org/10.1016/j.foodchem.2013.03.098>
- Tajika, A., Morimoto, N., & Landman, N. H. (2021). Significance of the suture line in cephalopod taxonomy revealed by 3D morphometrics in the modern nautilus *Nautilus* and *Allonautilus*. *Scientific Reports*, 11(1): 17114. <https://doi.org/10.1038/s41598-021-96611-1>

- Takiguchi, Y. (1991a). Advances in Chitin Science, Vol. III Proceedings from the third Asia-Pacific Chitin, Chitosan Jikken manual chapter 1. In Physical properties of chitinous materials (1st ed., Vol. 3, pp. 1–7). Gihodou Shupan Kaisha.
- Takiguchi, Y. (1991b). Chitin, Chitosan Jikken Manual Chapter-2. In Chitin, Chitosan Jikken Manual Chapter-2 (pp. 9–17). Gihodou Shupan Kaisha.
- Thirunavukkarasu, N., & Shanmugam, A. (2009). Extraction Of Chitin And Chitosan From Mud Crab *Scylla tranquebarica* (Fabricius, 1798). International Journal on Applied Bio-Engineering, 4(2): 31–33. <https://doi.org/10.18000/ijabeg.10048>
- Trung, T. S., Thein-Han, W. W., Qui, N. T., Ng, C.-H., & Stevens, W. F. (2006). Functional characteristics of shrimp chitosan and its membranes as affected by the degree of deacetylation. Bioresource Technology, 97(4): 659–663. <https://doi.org/10.1016/j.biortech.2005.03.023>
- Uğurlu, E., & Duysak, Ö. (2023). A study on the extraction of chitin and chitosan from the invasive sea urchin *Diadema setosum* from Iskenderun Bay in the Northeastern Mediterranean. Environmental Science and Pollution Research, 30(8): 21416–21424. <https://doi.org/10.1007/s11356-022-23728-9>
- Uğurlu, E., Duysak, Ö., Saygılı, İ., Uğur, S., & Sayın, S., (2020). Denizel Omurgasız Canlılardan Elde Edilen Kolajenler ve Kullanım Alanları. Ecological Life Sciences, 15(1):24-35, <https://doi.org/10.12739/NWSA.2020.15.1.5A0130>.
- Uğurlu, E., Duysak, Ö., & Ozcan, T. (2018). Consumer Behaviour of Cephalopod Consumption in Kilis City. 259–263.
- Ullah, R., & Khan, I. (2023). Biotechnological Utilization of the Marine Environment for Food, Drugs, and Energy (pp. 23–46). https://doi.org/10.1007/978-981-99-0624-6_2
- Vairamani, S., Subhapradha, N., Ramasamy, P., Raveendran, S., Srinivasan, A., & Shanmugam, A. (2013). Physicochemical Characteristics and Antioxidant Efficacy of Chitosan From The Internal Shell of Spineless Cuttlefish *Sepiella inermis*. Preparative Biochemistry and Biotechnology, 43(7): 696–716. <https://doi.org/10.1080/10826068.2013.773339>
- Vino, B., Ramasamy, P., Shanmugam, V., & Shanmugam, A. (2012). Extraction, characterization and in vitro antioxidative potential of chitosan and sulfated chitosan from Cuttlebone of *Sepia aculeata* Orbigny, 1848. Asian Pacific Journal of Tropical Biomedicine, 2: 334–341. [https://doi.org/10.1016/S2221-1691\(12\)60184-1](https://doi.org/10.1016/S2221-1691(12)60184-1)
- Vino, B., Ramasamy, P., Vairamani, S., & Shanmugam, A. (2011). Physicochemical characterization of biopolymers chitin and chitosan extracted from squid *Doryteuthis sibogae* Adam, 1954 pen. International Journal of Pharma Research and Development, 2.
- Xavier, J. C., Cherel, Y., Allcock, L., Rosa, R., Sabirov, R. M., Blicher, M. E., & Golikov, A. V. (2018). A review on the biodiversity, distribution and trophic role of cephalopods in the Arctic and Antarctic marine ecosystems under a changing ocean. Marine Biology, 165(5): 93. <https://doi.org/10.1007/s00227-018-3352-9>
- Xavier, J., & Cherel, Y. (2021). Cephalopod Beak Guide For the Southern Ocean: An update on taxonomy.
- Yen, M.-T., Yang, J.-H., & Mau, J.-L. (2009). Physicochemical characterization of chitin and chitosan from crab shells. Carbohydrate Polymers, 75(1): 15–21. <https://doi.org/10.1016/j.carbpol.2008.06.006>
- Younes, I., & Rinaudo, M. (2015). Chitin and Chitosan Preparation from Marine Sources. Structure, Properties and Applications. Marine Drugs, 13(3): 1133–1174. <https://doi.org/10.3390/md13031133>
- Yuan, Y., Chesnutt, B. M., Haggard, W. O., & Bumgardner, J. D. (2011). Deacetylation of Chitosan: Material Characterization and in vitro Evaluation via Albumin Adsorption and Pre-Osteoblastic Cell Cultures. Materials, 4(8): 1399–1416. <https://doi.org/10.3390/ma4081399>
- Žigayová, D., Mikušová, V., & Mikuš, P. (2023). Advances in Antiviral Delivery Systems and Chitosan-Based Polymeric and Nanoparticulate Antivirals and Antiviral Carriers. Viruses, 15(3): 647. <https://doi.org/10.3390/v15030647>

Tables

Table 1. Comparison of significant peak wave numbers in the FTIR spectrum of CT obtained from the dorsal fin of *S. officinalis* and commercial CT.

Functional group and vibration modes (Pearson et al., 1960)	Commercial CT peak wavenumber (cm ⁻¹)	Cuttlebone CT peak wavenumber (cm ⁻¹)
OH out of plane bending	690	699.07
CH ring stretching	896	856.24
CH ₃ wagging	952	956.51
C–O asymmetric stretch in phase ring	1024	1027.87
C–O–C asymmetric stretch in phase ring	1068	1063.55
Asymmetric in-phase ring stretching mode	1114	1113.69
Asymmetric bridge oxygen stretching	1155	1154.19
CH ₂ ending and CH ₃ deformation	1430	1443.45
C–O secondary amide stretch	1620	1639.19
C–O secondary amide stretch	1654	1659.45
CH ₃ symmetrical stretch	2867	2882.09
CH ₃ symmetrical stretch and CH ₂ asymmetric stretch	2937	2938.98
N–H stretching	3101-3259	3282.25
O–H stretching	3437	3407.61
References	Kaya et al. (2015)	This study

Table 2. Comparison of significant peak wavenumbers in the FTIR spectrum of CS obtained from the cuttlebone of *S. officinalis* and commercial CS.

Functional group and vibration mode	Commercial CS peak wavenumber (cm ⁻¹)	CS from Cuttlebone peak wavenumber (cm ⁻¹)
Pyranose ring skeletal vibrations	892	871.66
ν (C–O) in primary OH group	985	989.30
ν (C–O) in secondary OH group	1021	1028.84
ν_{as} (C–O–C) (glycosidic linkage)	1062	1083.79
ν_s (C–O–C) (glycosidic linkage)	1149	1155.15
Complex vibrations of NHCO group (amide III band)	1258	1227.47

δ (C–H) in pyranose ring	1317	1311.46
δ_s (CH ₃) in NHCOCH ₃ group	1375	1396.21
δ (CH ₂) in CH ₂ OH group	1420	1443.45
ν (NH ₂) in NHCOCH ₃ group (amide II band)	1586	1593.87
ν (C=O) in NHCOCH ₃ group (amide I band)	1652	1652.69
ν (C–H) in pyranose ring	2871	2851.24
ν_{as} (CH ₂) in CH ₂ OH group	2921	2938.02
ν (NH ₂) associated with primary amines and OH associated with pyranose ring	3356	3352.63
References	Kaya et al. (2013)	This study

Figures



Figure 1. Cuttlebone of *S. officinalis* and after grinding process.

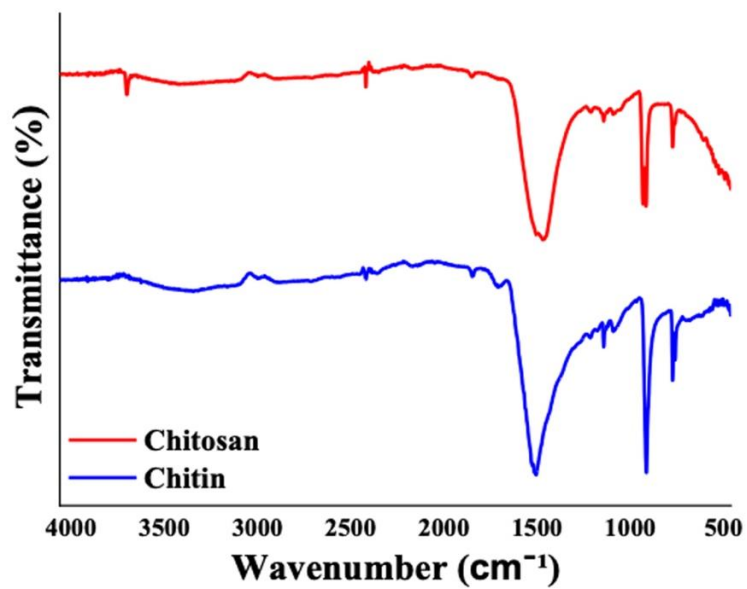


Figure 2. FTIR bands of chitin (CT) and chitosan (CS) from cuttlebone of *S. officinalis*.

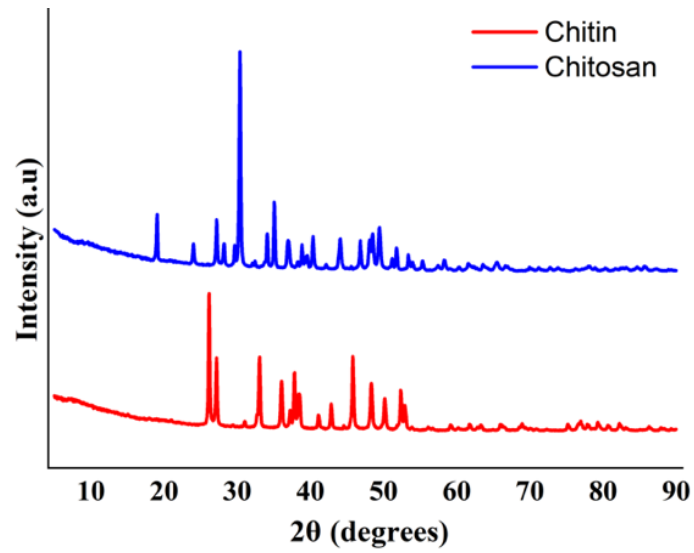


Figure 3. Comparison of X-ray power diffractograms of chitin (CT) and chitosan (CS) from cuttlebone of *S. officinalis*.

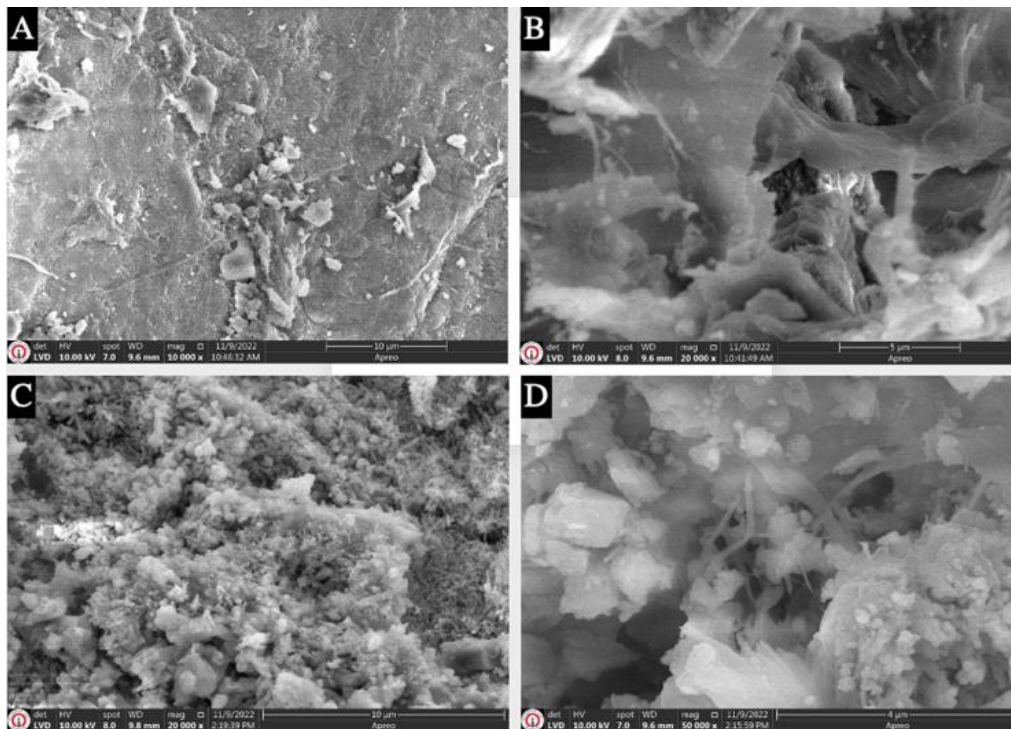


Figure 4. SEM images of chitin (CT) and chitosan (CS) from cuttlebone of *Sepia officinalis*: A, B) CT from cuttlebone, C, D) CS from cuttlebone.